

Y.A. Bhagat  
D.J. Emery  
S. Naik  
T. Yeo  
C. Beaulieu

# Comparison of Generalized Autocalibrating Partially Parallel Acquisitions and Modified Sensitivity Encoding for Diffusion Tensor Imaging

**BACKGROUND AND PURPOSE:** Diffusion tensor magnetic resonance imaging (DTI) of the brain is usually acquired with single-shot echo-planar imaging, which is associated with localized signal loss, geometric distortions, and blurring. Parallel imaging can lessen these artifacts by shortening the length of the echo-train acquisition. The self-calibrating parallel acquisition techniques, image domain-based modified sensitivity encoding (mSENSE) and *k*-space-based generalized autocalibrating partially parallel acquisitions (GRAPPA), were evaluated with DTI of the brain in 5 healthy subjects.

**METHODS:** GRAPPA and mSENSE with higher acceleration factors (*R*) up to 4 were compared with conventional DTI (with and without phase partial Fourier, another method of reducing the echo-train length) on a 1.5T Sonata scanner (Siemens, Erlangen, Germany). The resulting images and diffusion maps were evaluated qualitatively and quantitatively. Qualitative analysis was performed by 3 reviewers blinded to the technique using image sharpness and the level of artifacts as characteristics for scoring each set of images. Quantitative comparisons encompassed measuring signal-to-noise ratio, Trace/3 apparent diffusion coefficient (ADC), and fractional anisotropy (FA) in 6 white-matter (WM) and gray-matter (GM) regions.

**RESULTS:** Reviewers scored the GRAPPA and mSENSE *R* = 2 images better than images acquired with conventional techniques. FA contrast was improved at the GM/WM junction in peripheral brain areas. Trace/3 ADC and FA measurements were consistent for all methods. However, *R* = 3,4 images suffered from reconstruction-related artifacts.

**CONCLUSIONS:** GRAPPA and mSENSE (*R* = 2) minimized the susceptibility and off-resonance effects associated with conventional DTI methods, yielding high-quality images and reproducible quantitative diffusion measurements.

Parallel acquisition techniques (PAT), when combined with single-shot echo-planar imaging (EPI) methods, can ameliorate artifacts such as signal intensity drop-out, gross geometric distortions, and blurring due to lengthy echo trains and T2\* decay associated with the EPI readout interval. In the case of conventional diffusion-weighted EPI, such artifacts lead to image degradation mainly at the base of the skull, in infratentorial aspects of the brain, and around the auditory canals or frontal sinuses, potentially impeding the accurate detection of ischemic lesions in diseases such as stroke.<sup>1-4</sup> Parallel imaging uses the spatial information from arrays of radio frequency (RF) coils to perform some portion of the spatial encoding normally accomplished by using gradients.<sup>5</sup> The benefits are accelerated image acquisition (ie, shorter echo-train length for EPI) because of a reduction in the number of

phase-encoding steps that need to be acquired, diminution of imaging artifacts, and resolution enhancement. A more common approach for accelerating image acquisition is the phase partial Fourier (PPF) method,<sup>6</sup> which samples *k*-space asymmetrically and thereby decreases the amount of phase-encoding steps required, albeit with artifacts incurred as a result of phase errors and penalties in signal-to-noise ratio (SNR). However, for both PAT and PPF, some SNR can be regained by using shorter spin-echo times.<sup>7,8</sup>

The image domain-based technique sensitivity encoding (SENSE),<sup>9</sup> when used with single-shot EPI-based diffusion tensor imaging (DTI) of the brain, yielded images with improved spatial resolution and reduced geometric distortions at 1.5T (with *R* = 2)<sup>10</sup> and 3T (with *R* = 2.4 and 3).<sup>7,8</sup> These aforementioned studies also used PPF of 60%–80% with all DTI scans. However, the impact of these SENSE-related benefits on the quantitative measures derived from DTI [Trace/3 apparent diffusion coefficient (ADC) and fractional anisotropy (FA)] was not determined relative to the conventional DTI technique. Furthermore, to our knowledge, there are no published systematic evaluations of the newer self-calibrating parallel imaging methods, modified SENSE (mSENSE)<sup>11</sup> or the *k*-space-based generalized autocalibrating partially parallel acquisitions (GRAPPA)<sup>12</sup> with DTI. Like SENSE, mSENSE accelerates imaging by undersampling *k*-space and generating reduced FOV or aliased images. By using the spatial information inherent in each receiver coil in the form of coil sensitivity maps, the image reconstruction process then effectively unfolds the aliased image.<sup>9,11</sup> However, for SENSE, coil sensitivity maps are calibrated from a separate scan, whereas for

Received November 16, 2005; accepted after revision March 22, 2006.

From the Departments of Biomedical Engineering (Y.A.B., D.J.E., C.B.) and Radiology and Diagnostic Imaging (D.J.E., S.N., T.Y.), University of Alberta, Edmonton, Alberta, Canada.

This work was supported by the Heart and Stroke Foundation of Alberta, Northwest Territories and Nunavut, Alberta Heritage Foundation for Medical Research, and the Canadian Institutes of Health Research (CIHR), as well as a "Focus on Stroke" doctoral training award (to Y.A.B.) from the Canadian Stroke Network, Heart and Stroke Foundation of Canada, CIHR, and AstraZeneca. The NMR facility infrastructure was provided by the Alberta Heritage Foundation for Medical Research, Alberta Science and Research Authority, University of Alberta Hospital Foundation, and Canada Foundation for Innovation.

Previously presented in part at 12th Annual Scientific Meeting of the International Society for Magnetic Resonance in Medicine (ISMRM), May 15–21, 2004, Kyoto, Japan; and 2nd ISMRM Workshop on Methods for Quantitative Diffusion MRI of Human Brain, March 13–15, 2005, Lake Louise, AB, Canada.

Address correspondence to Christian Beaulieu, PhD, Department of Biomedical Engineering Faculty of Medicine and Dentistry, University of Alberta, 1098 Research Transition Facility, Edmonton, AB T6G 2V2, Canada; e-mail: christian.beaulieu@ualberta.ca

**Acquisition times and echo times (TE) for conventional DTI with and without PPF and mSENSE- or GRAPPA-based DTI sequences with varying acceleration factors (R)**

Acceleration Factor	Conventional DTI (R = 1)		Parallel Imaging with no PPF		
	With PPF (6/8)	Without PPF	R = 2	R = 3	R = 4
Acquisition time (minutes:seconds)	2:44	3:10	2:55	3:01	3:04
TE (ms)	82	107	81	76	71

**Note:**—TR was kept constant at 2.8 seconds for DTI with PPF and parallel imaging, whereas it was 3.3 seconds for DTI without PPF. DTI indicates diffusion tensor imaging; PPF, phase partial Fourier; mSENSE, modified sensitivity encoding; GRAPPA, generalized autocalibrating partially parallel acquisitions.

mSENSE, sensitivity map calibration is performed by acquiring extra lines within the accelerated acquisition itself that are not included in the final image reconstruction, a property defined as autocalibration. GRAPPA also employs autocalibration, but here the missing lines of *k*-space for final image reconstruction are calculated from the small amount of acquired lines in the *k*-space domain, before Fourier transformation of the data.<sup>12</sup> Besides, in GRAPPA, the extra lines acquired for coil sensitivity calibration can be integrated into the final reconstruction to reduce the effects of any residual aliasing artifacts that may be present.<sup>13,14</sup>

Previous studies comparing mSENSE and GRAPPA for various applications other than DTI have concluded that GRAPPA was superior to mSENSE in terms of image quality, SNR, and restricting aliasing artifacts for true free induction with steady-state precession (FISP) sequences in cardiac cine imaging,<sup>15</sup> and T2-weighted turbo spin-echo sequences in lumbar spine imaging.<sup>16</sup> However, 1 study noted significant merits of mSENSE over GRAPPA with respect to image quality and lesion conspicuity in the case of 3D volume-interpolated breath-hold examinations for liver imaging.<sup>17</sup> The purpose of our study was to compare the qualitative aspects of the images and quantitative diffusion parameters obtained with mSENSE- and GRAPPA-based DTI with higher acceleration factors (up to R = 4, no PPF) versus conventional DTI with and without PPF. A rectangular FOV with right-left phase encoding was used to further reduce the echo-train length and capitalize on shorter echo times for gains in SNR. We hypothesized that both GRAPPA and mSENSE would improve the conspicuity of detailed image features and generate more reliable quantitative Trace/3 ADC and FA values, especially in regions compromised by the common EPI-related artifacts.

**Materials and Methods**

Images were obtained from a group of 5 healthy subjects (mean age, 28 ± 3 years). DTI was performed on a 1.5T Magnetom Sonata scanner (Siemens Medical Systems, Erlangen, Germany) equipped with gradient coils producing maximal amplitude of 40 mT/m and slew rate of 200 T/m/s. An 8-channel phased array RF coil (In Vivo, Orlando, Fla) was used with conventional DTI (R = 1) with and without PPF, and mSENSE DTI and GRAPPA DTI without PPF (commercial parallel imaging software, Siemens 2004A). Conventional single-shot spin-echo diffusion EPI (R1-no PPF) used: TR/TE/NEX = 3.3 seconds/107 ms/8; matrix, 96 × 128; rectangular FOV, 195 × 260 mm; 20 3-mm contiguous axial sections; bandwidth of 1446 Hz/pixel; echo spacing of 0.8 ms; right-left phase encode direction; scan time, 3 minutes and 10 seconds.

The diffusion tensor was acquired with diffusion gradients along 6 noncollinear directions {b = 1000 s/mm<sup>2</sup>; (X, Y, Z) gradient directions = (1, 0, 1) (-1, 0, 1), (0, 1, 1) (0, 1, -1), (1, 1, 0) (-1, 1, 0)} and one scan without diffusion weighting (b = 0 s/mm<sup>2</sup>, b0). DTI data

were reacquired for R1 with PPF (6/8) and R = 2, 3, and 4 for both mSENSE and GRAPPA without PPF (24 reference lines). To better compare results from the 2 image acceleration methods (ie, PPF and parallel imaging), PPF was not incorporated with parallel imaging-based DTI sequences. The geometric acquisition parameters, number of averages (8), and TR (2.8 seconds) were kept constant for these sequences, and TE was minimized for each value of R as shown in the Table. The TR was kept constant to avoid any T1-discriminating effects that might arise from implementing an effectively lower TR for the parallel imaging methods (R = 2–4). TR could have been reduced by 0.3–0.8 seconds relative to R1-PPF. The constant number of averages permitted a clinically reasonable acquisition time for each sequence. A 2-L nickel-doped water bottle was used as an isotropic phantom (n = 5). DTI measurements were repeated on a single volunteer (n = 4) over a 1-week period to evaluate the stability of diffusion metrics in vivo for conventional DTI and mSENSE- and GRAPPA-based DTI. Trace/3 ADC and FA maps were generated using MRVision image analysis software (Winchester, Mass).

The b0 and b1000 images and Trace/3 ADC and FA maps of all 5 subjects were reviewed by a group of 3 experienced neuroradiologists (D.J.E, S.N., T.Y.) blinded to the method used (GRAPPA, mSENSE, R1-PPF, or R1-no PPF) and its acquisition parameters. A group consensus was reached with regard to the quality of the images with each set of images ranked from 1 to 4 (1 was the best and 4 was the worst). Image sharpness and presence or absence of artifacts within the brain were the 2 characteristics most useful in differentiating between images acquired with the different methods.

The SNR was calculated on b0 images according to a modification of the dual acquisition subtraction method<sup>18,19</sup> proposed by Reeder et al<sup>20</sup> for magnitude images acquired with parallel imaging. Two sequential acquisitions of identical images S<sub>1</sub> and S<sub>2</sub> were acquired in this method. An estimate of the mean signal intensity was obtained from a region of interest (ROI) from the sum of S<sub>1</sub> and S<sub>2</sub>. The SD of the difference within the same region of interest was obtained from the subtraction of one image from the other. The SNR was calculated according to

$$1) \quad SNR = \frac{\text{mean}(S_1 + S_2)}{\sqrt{2} \text{SD}(S_1 - S_2)}$$

Due to the varying noise profile of accelerated images, the SNR, neglecting the effect of autocalibrating lines, is given by<sup>9,20</sup>:

$$2) \quad SNR_{PAT} = \frac{SNR_{full}}{g \sqrt{R}}$$

where SNR<sub>full</sub> is the SNR of the conventional image, and g is the geometry or g-factor that describes the noise enhancement across the image for a given coil configuration. The g-factor depends on the spatial location within the image, the R factor, and the geometric properties of a specific coil array. Based on these features, the measurement of noise in a region different from that of the signal intensity measurement can lead to incorrect interpretations of regional SNR.

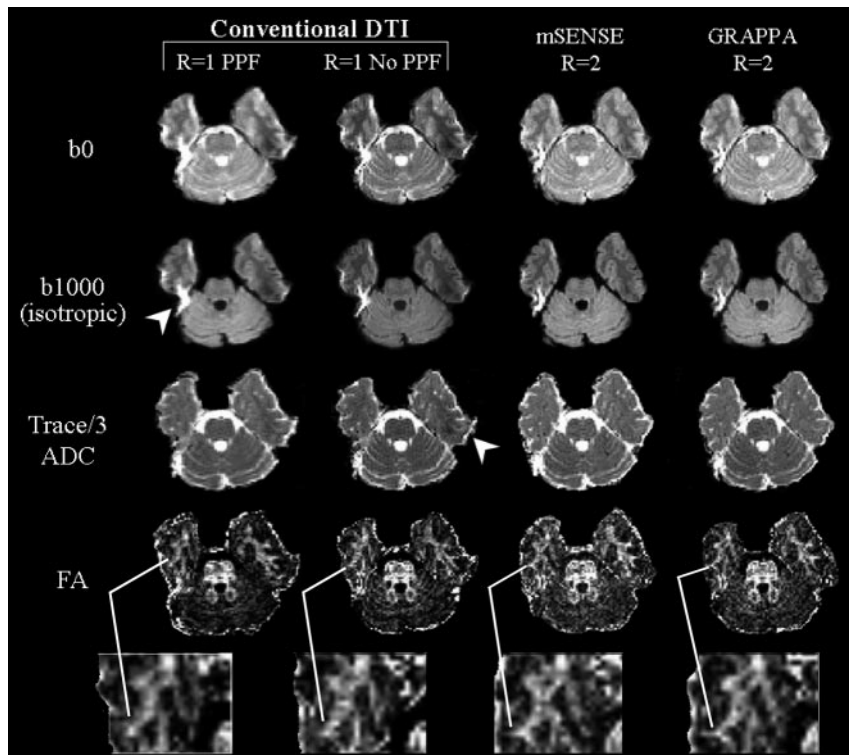


**Fig 1.** Representative sets of  $b_0$  (T2-weighted),  $b_{1000}$  (isotropic diffusion weighted) images, and Trace/3 ADC and FA maps of one inferior section (level of pons) from one subject with conventional ( $R = 1$ ), and mSENSE and GRAPPA  $R = 2$  based DTI. Compared with R1-PPF and R1-no PPF, a reduction in distortions and off-resonance effects (arrowheads) are apparent with images obtained with mSENSE and GRAPPA  $R = 2$  DTI. Although FA maps obtained with R1-PPF were deemed to be the best in 4 of 5 subjects based on their higher SNR and smoother profiles (qualitative analysis by neuroradiologists), closer inspection showed that peripheral white matter structures such as the middle temporal gyrus (magnified, below FA maps) affected by the distortions with conventional DTI were better resolved with the mSENSE and GRAPPA  $R = 2$  based DTI methods.

DTI). Results from evaluation of the FA maps were less consistent and contrary to that of the  $b_0$  and diffusion images and Trace/3 ADC maps. FA maps of the R1-PPF technique were found to be superior in 4 of the 5 subjects. This technique generally provided the best overall FA map of both subcortical and deep WM in terms of sharpness and contrast relative to the background GM. However, closer inspections of the FA maps obtained with parallel imaging demonstrated fewer distortions, especially for

basal structures and yielded better-defined WM regions as seen on magnified sections of the FA maps. Our qualitative findings are in good agreement with previous studies.<sup>7,10,21,22</sup>

Images acquired with higher acceleration factors ( $R = 3$  and 4) suffered from pernicious reconstruction artifacts, such as aliasing and structural noise enhancement as apparent in the postprocessed Trace/3 ADC and FA maps (Fig 3), thereby precluding their use for the previous qualitative analysis or the hindered performance of these techniques at higher  $R$  factors relate to nonideal conditioning in reconstruction, leading to localized noise enhancement in the unfolded images for mSENSE or inaccuracies in calculations of missing  $k$ -space lines, which generate aliasing in the case of GRAPPA.<sup>13</sup> Furthermore, in GRAPPA, incorporating a single-shot EPI calibration scan (for derivation of coil weights) in the actual DTI sequence, as opposed to performing a separate scan, may cause artifacts because of an incompatibility with the applied diffusion encoding gradients.<sup>5</sup> Our results are specific to our current implementation of parallel imaging, which is an evolving field on its own, and vary from previous reports that have demonstrated high-quality DTIs of the brain with SENSE  $R = 3$ ,<sup>7,22</sup> which, unlike mSENSE, obtains sensitivity maps from separate calibration scans.

From a quantitative perspective, we observed elevations of mean FA with R1-no PPF ( $0.05 \pm 0.01$ ), mSENSE  $R = 2$  ( $0.08 \pm 0.01$ ), and GRAPPA  $R = 2$  ( $0.07 \pm 0.01$ ) relative to R1-PPF ( $0.04 \pm 0.01$ ) in an isotropic water phantom (Fig 4A). However, Trace/3 ADC values in the phantom fluctuated to a lesser extent (3%) when comparing R1-PPF to R1-no PPF and GRAPPA  $R = 2$ , and comparing R1-no PPF to mSENSE and GRAPPA  $R = 2$  (Fig 4B). The elevations in FA encountered with parallel imaging relative to conventional DTI are not unexpected given the known noise-induced bias in FA quantifi-

## Results and Discussion

Region of interest analysis of 6 different regions per subject were stratified according to their respective range of FA values into categories such as the major white matter (WM) tracts (genu and splenium of corpus callosum,  $FA = 0.67-0.76$ ), subcortical WM (superior temporal gyrus and middle temporal gyrus,  $FA = 0.44-0.47$ ), and cortical gray matter (GM) (GM regions adjacent to the 2 gyri mentioned above,  $FA = 0.16-0.19$ ). The ROI traces encompassed the full visible outline of the structure on one 2D section and were cross-referenced with  $b_0$  images to avoid inclusion of obviously visible CSF-filled spaces. To account for effects of spatial warping primarily at the edges of peripheral structures and at the basal levels of the brain, and to avoid ensuing partial volume averaging with neighboring tissues, the ROIs were consistently either repositioned or redrawn for images of the conventional and parallel imaging methods. Paired  $t$  tests were used for statistical analysis of SNR and Trace/3 ADC and FA obtained from conventional DTI ( $R = 1$ ) versus mSENSE DTI and GRAPPA DTI. The reproducibility of quantitative diffusion for R1-PPF and mSENSE  $R = 2$  and GRAPPA  $R = 2$  were assessed by repeated measurements for a single subject over 4 scans and showed up to a 4% variation in FA and 5% in Trace/3 ADC in the genu of the corpus callosum (data not shown).

In the qualitative image analysis, the  $b_0$ ,  $b_{1000}$ , and Trace/3 ADC images were evaluated as a group, whereas the FA maps were evaluated separately. For the  $b_0$ ,  $b_{1000}$ , and Trace/3 ADC group, images acquired using mSENSE  $R = 2$  were consistently found to be the best in all 5 subjects, followed by those obtained using GRAPPA  $R = 2$  (both without PPF) (Figs 1 and 2). Images derived using R1-PPF and R1-no PPF were found to be poorer in quality for all cases. GRAPPA and mSENSE  $R = 2$  images appeared sharper and were less vulnerable to typical EPI artifacts and blurring observed in images acquired with the more commonplace R1-PPF method (ie, "standard"

From a quantitative perspective, we observed elevations of mean FA with R1-no PPF ( $0.05 \pm 0.01$ ), mSENSE  $R = 2$  ( $0.08 \pm 0.01$ ), and GRAPPA  $R = 2$  ( $0.07 \pm 0.01$ ) relative to R1-PPF ( $0.04 \pm 0.01$ ) in an isotropic water phantom (Fig 4A). However, Trace/3 ADC values in the phantom fluctuated to a lesser extent (3%) when comparing R1-PPF to R1-no PPF and GRAPPA  $R = 2$ , and comparing R1-no PPF to mSENSE and GRAPPA  $R = 2$  (Fig 4B). The elevations in FA encountered with parallel imaging relative to conventional DTI are not unexpected given the known noise-induced bias in FA quantifi-

From a quantitative perspective, we observed elevations of mean FA with R1-no PPF ( $0.05 \pm 0.01$ ), mSENSE  $R = 2$  ( $0.08 \pm 0.01$ ), and GRAPPA  $R = 2$  ( $0.07 \pm 0.01$ ) relative to R1-PPF ( $0.04 \pm 0.01$ ) in an isotropic water phantom (Fig 4A). However, Trace/3 ADC values in the phantom fluctuated to a lesser extent (3%) when comparing R1-PPF to R1-no PPF and GRAPPA  $R = 2$ , and comparing R1-no PPF to mSENSE and GRAPPA  $R = 2$  (Fig 4B). The elevations in FA encountered with parallel imaging relative to conventional DTI are not unexpected given the known noise-induced bias in FA quantifi-

From a quantitative perspective, we observed elevations of mean FA with R1-no PPF ( $0.05 \pm 0.01$ ), mSENSE  $R = 2$  ( $0.08 \pm 0.01$ ), and GRAPPA  $R = 2$  ( $0.07 \pm 0.01$ ) relative to R1-PPF ( $0.04 \pm 0.01$ ) in an isotropic water phantom (Fig 4A). However, Trace/3 ADC values in the phantom fluctuated to a lesser extent (3%) when comparing R1-PPF to R1-no PPF and GRAPPA  $R = 2$ , and comparing R1-no PPF to mSENSE and GRAPPA  $R = 2$  (Fig 4B). The elevations in FA encountered with parallel imaging relative to conventional DTI are not unexpected given the known noise-induced bias in FA quantifi-



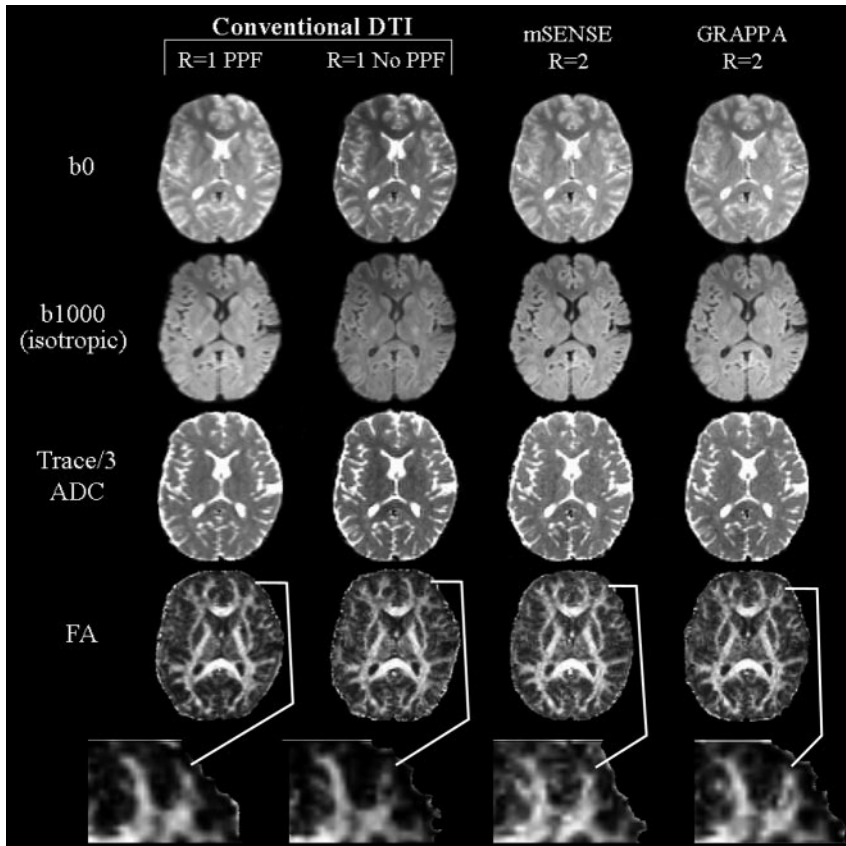


**Fig 2.** Image sets ( $b_0$ ,  $b_{1000}$ ) and Trace/3 ADC and FA maps of a middle section (level of corpus callosum) from one subject with conventional ( $R = 1$ ), and mSENSE and GRAPPA  $R = 2$  based DTI. Qualitative analysis of the  $b_0$  and  $b_{1000}$  images, and Trace/3 ADC maps indicated that mSENSE and GRAPPA  $R = 2$  DTI generated the sharpest images and were more adept at handling spatial warping effects seen in images of the R1-PPF and R1-no PPF methods. Although FA maps derived from R1-PPF were considered to be smoother because of their intrinsically higher SNR in 4 of 5 cases, an in-depth comparison of these maps to those obtained by using mSENSE and GRAPPA  $R = 2$  DTI showed that incorporating parallel imaging allowed better visualization of thinner white matter tracts such as the middle frontal gyrus (*magnified, below FA maps*).

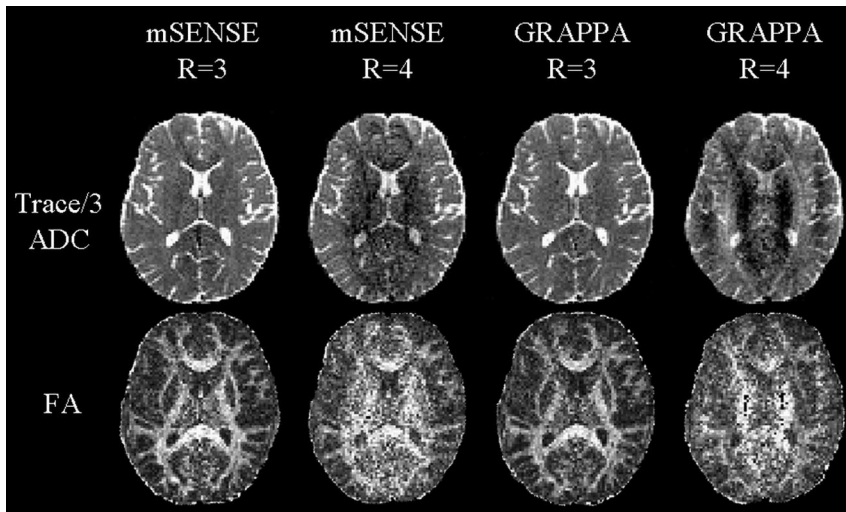


**Fig 3.** Poor quality Trace/3 ADC and FA maps of one middle section (level of corpus callosum) from one subject using mSENSE and GRAPPA  $R = 3$  and 4-based DTI. Maps obtained from mSENSE  $R = 4$ , and GRAPPA  $R = 3, 4$  suffered from reconstruction artifacts such as aliasing and were not considered for quantitative analysis. Trace/3 ADC maps from mSENSE  $R = 3$  revealed regions with enhanced noise centrally and were also excluded from further analysis.

cation, particularly at low FA values.<sup>23</sup> Fig 5 displays a plot of mean relative SNR values ( $R2/R1$ -PPF) for the phantom and 3 brain regions in 5 subjects. Although we expect only a  $\sqrt{2}$  loss in SNR with parallel imaging under ideal conditions for  $g = 1.0$ ,<sup>9</sup> the steeper declines in relative SNR with mSENSE and GRAPPA  $R = 2$  are due to the higher SDs (mSENSE  $\cong 17$ , GRAPPA  $\cong 15$ ) relative to R1-PPF ( $\sim 6$ ) measured in ROIs from the difference images of those methods. This is a result of noise enhancement, which may be a consequence of the variations in the  $g$ -factor owing to coil configuration or section location with respect to elements of the coil array.<sup>9</sup> Others have noted that enhancing the distance between the phantom or subjects and the coil

elements can moderate the steep variance in coil-sensitivity profiles proximal to the coil and limit errors in image reconstruction, thereby optimizing image quality and refining SNR.<sup>1</sup> In our study, although this feature was easy to implement for the smaller cylindrical phantom, it was not feasible for an adult human head relative to the sensitive volume of the coil (24 cm).

FA values in vivo remained fairly consistent for all acquisition methods, revealing small increases for the mSENSE  $R = 2$  technique of up to 5% for the corpus callosum and subcortical WM (Fig 4A). Using R1-PPF as the basis of comparison, the Trace/3 ADC values were observed to fluctuate with decreases (4%–17%) for R1-no PPF and increases (4%–7%) for the

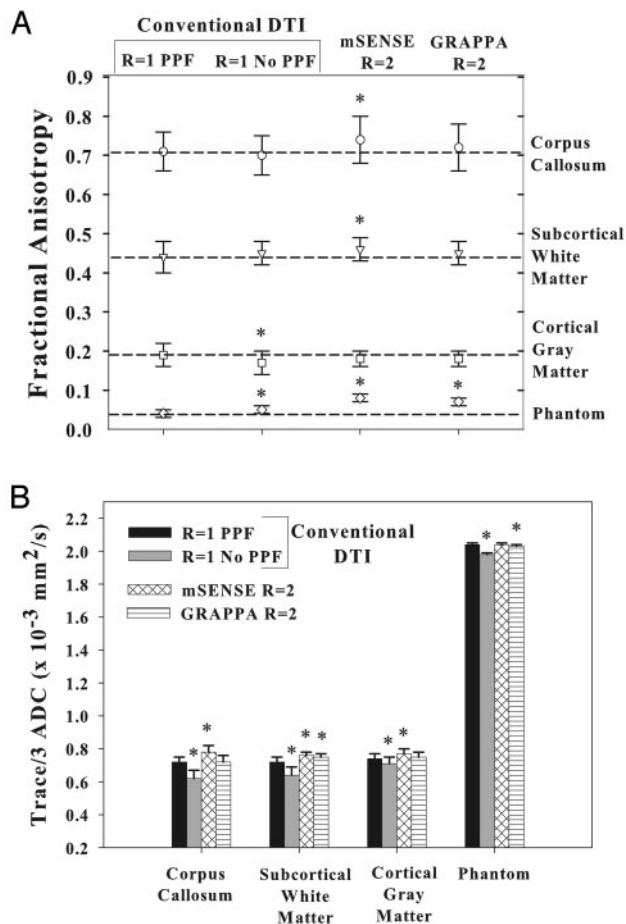


**Fig 4.** Fractional anisotropy (FA) and Trace/3 ADC (B) values (mean ± SD) for 3 brain regions in 5 normal subjects using conventional DTI R1-PPF, R1-no PPF, and mSENSE and GRAPPA R = 2 DTI methods. The dashed lines in A indicate FA values obtained with conventional R1-PPF for different structures and help demonstrate the extent of variations with measurements made by using other techniques. Although subtle differences are evident, the values appear to be fairly consistent between parallel imaging and conventional DTI. Values for mSENSE and GRAPPA R = 3, 4 methods are not shown because of the poor quality of the maps. \* indicates significant ( $P < .05$ ) paired differences of R1-PPF versus R1-no PPF, mSENSE R = 2, and GRAPPA R = 2 methods.

mSENSE R = 2 and GRAPPA R = 2 methods for the corpus callosum, subcortical WM, and cortical GM areas (Fig 4B). Although our normative FA values for R1-PPF based DTI (the pseudo-“gold standard”) are in firm agreement with those published previously,<sup>24</sup> recent PAT-based DTI studies of the brain do not mention in vivo FA values,<sup>7,10,21,22</sup> limiting our ability to draw comparisons between their data and our mSENSE and GRAPPA R = 2 derived measures. Mean SNR values measured by using the R1-PPF method ranged from 35–45 in the corpus callosum, subcortical WM, and cortical GM. Overall, relative SNR ( $SNR_{PAT(R2)}/SNR_{R1-PPF}$ ) was reduced to a greater extent in central structures (such as the corpus callosum) compared with peripheral structures (such as subcortical WM) (Fig 5) and is probably responsible for the small systematic changes in the diffusion parameters obtained with parallel imaging. However, in a separate study in which we performed mSENSE and GRAPPA R = 2 DTI with 16 averages and compared the data with that from R1-PPF and R1-no PPF with 8 averages in 4 subjects, the results were no different, suggesting that

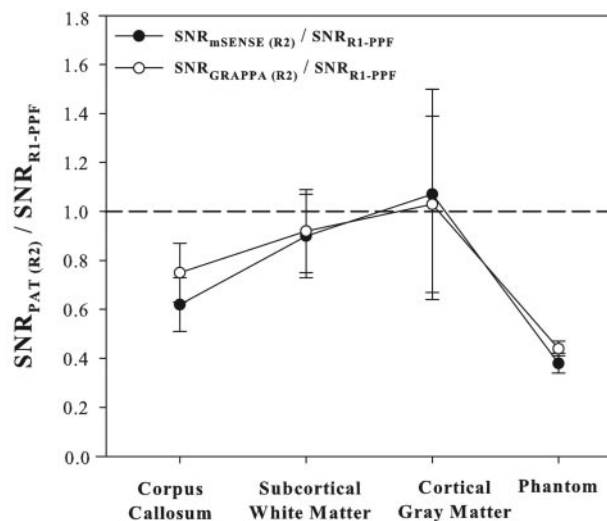


**Fig 5.** Relative (parallel acquisition technique [PAT] R = 2 / R1-PPF) signal-to-noise ratio (SNR) measurements (mean ± SD) of mSENSE or GRAPPA R = 2 for 3 brain regions in 5 normal subjects. SNR values were fairly close between mSENSE and GRAPPA R = 2 methods for the 3 structures evaluated. Relative SNR values were reduced by 25%–38% and 8%–10% in the corpus callosum and subcortical white matter in the gyri. Cortical gray matter demonstrated relative SNR values closer to unity with a higher percentage of error (35%–40%) in the measurements. Relative SNR values in the phantom decreased by 56% and 62% for the GRAPPA and mSENSE R = 2 methods, respectively, in accordance with theoretical considerations reflecting higher (>1.0) coil *g*-factors.<sup>9</sup>

alterations in Trace/3 ADC and FA are not entirely SNR-dependent (data not shown).

Our choice of the right-left phase encoding direction with a rectangular FOV of 75% enabled a faster *k*-space traversal and reduction in echo-train length, which yielded gains in SNR and marked reductions in geometric distortions in the frontal regions of the brain that are synonymous with anteroposterior phase encoding with a square FOV.<sup>1</sup> Our results would translate well to single-shot, EPI-based DTI at higher fields (3T and above) because the common EPI-related susceptibility artifacts and T2\* blurring seen here are more pronounced at high field and can be minimized by use of parallel imaging.<sup>7,8</sup> Furthermore, in addition to gaining SNR from significant reductions in TE as a result of the shorter echo-train length, parallel imaging can confer enhancements in resolution (Fig 1 and 2) and yield improved anatomic detail for more precise Trace/3 ADC and FA measures. Unlike earlier studies,<sup>7,8,10</sup> our study did not incorporate PPF into parallel imaging based DTI for further comparisons. However, to test the effects of PPF on PAT, we performed mSENSE and GRAPPA DTI with 6/8 PPF (R/L phase encoding) for acceleration factors up to 4 in 1 subject. The use of PPF resulted in a shorter TE of 72, 68, and 67 ms for R = 2, 3, and 4, respectively. Nonetheless, image and diffusion map quality, though acceptable with R2-PPF, suffered from blurring and lack of sharpness (data not shown) compared with the R2-no PPF images in the present study. It is important to note that the differences between conventional and parallel imaging-based DTI can be more dramatic when the image acquisition uses purely axial sections rather than obliques, anteroposterior phase encoding without rectangular FOV, larger matrix, and fields higher than 1.5T.

## Conclusion

We have shown images and Trace/3 ADC and FA maps of good quality with mSENSE and GRAPPA R = 2 based DTI at 1.5T. Improvements in FA contrast at borders between GM and WM regions were primarily observed in peripheral brain areas. Despite decreases in SNR, the parallel imaging methods addressed issues of susceptibility and off-resonance artifacts noted with conventional DTI (R1-PPF and R1-no PPF) and yielded higher quality images. Quantitative Trace/3 ADC and FA measurements were accurate and reproducible with both parallel imaging methods with an acceleration factor of 2.

## Acknowledgments

We thank Roland Bammer from the Lucas MRI Center, Stanford University, and David Porter, Gunnar Krueger, and Stephan Kannengiesser from Siemens Medical Solutions, Erlangen, Germany, for their invaluable expertise on implementation issues. We also acknowledge Richard Thompson from the University of Alberta for stimulating discussions on image reconstruction and SNR measurements with parallel acquisition techniques.

## References

1. Bammer R, Keeling SL, Augustin M, et al. **Improved diffusion-weighted single-shot echo-planar imaging (EPI) in stroke using sensitivity encoding (SENSE).** *Magn Reson Med* 2001;46:548–54
2. Willinek WA, Gieseke J, von Falkenhausen M, et al. **Sensitivity encoding for fast MR imaging of the brain in patients with stroke.** *Radiology* 2003;228:669–75
3. Augustin M, Fazekas F, Bammer R. **Fast patient workup in acute stroke using parallel imaging.** *Top Magn Reson Imaging* 2004;15:207–19
4. Kuhl CK, Gieseke J, von Falkenhausen M, et al. **Sensitivity encoding for diffusion-weighted MR imaging at 3.0 T: intraindividual comparative study.** *Radiology* 2005;234:517–26
5. Bammer R, Schoenberg SO. **Current concepts and advances in clinical parallel magnetic resonance imaging.** *Top Magn Reson Imaging* 2004;15:129–58
6. McGibney G, Smith MR, Nichols ST, et al. **Quantitative evaluation of several partial Fourier reconstruction algorithms used in MRI.** *Magn Reson Med* 1993;30:51–59
7. Jaermann T, Crelier G, Pruessmann KP, et al. **SENSE-DTI at 3 T.** *Magn Reson Med* 2004;51:230–36
8. Jaermann T, Pruessmann KP, Valavanis A, et al. **Influence of SENSE on image properties in high-resolution single-shot echo-planar DTI.** *Magn Reson Med* 2006;55:335–42
9. Pruessmann KP, Weiger M, Scheidegger MB, et al. **SENSE: sensitivity encoding for fast MRI.** *Magn Reson Med* 1999;42:952–62
10. Bammer R, Auer M, Keeling SL, et al. **Diffusion tensor imaging using single-shot SENSE-EPI.** *Magn Reson Med* 2002;48:128–36
11. Wang J, Kluge T, Nittka M, et al. **Parallel acquisition techniques with modified SENSE reconstruction mSENSE.** *Proceedings of the first Wurzburg workshop on parallel imaging basics and clinical applications.* Wurzburg, Germany;2001:89
12. Griswold MA, Jakob PM, Heidemann RM, et al. **Generalized autocalibrating partially parallel acquisitions (GRAPPA).** *Magn Reson Med* 2002;47:1202–10
13. Blaimer M, Breuer F, Mueller M, et al. **SMASH, SENSE, PILS, GRAPPA: how to choose the optimal method.** *Top Magn Reson Imaging* 2004;15:223–36
14. Griswold MA, Kannengiesser S, Heidemann RM, et al. **Field-of-view limitations in parallel imaging.** *Magn Reson Med* 2004;52:1118–26
15. Hunold P, Maderwald S, Ladd ME, et al. **Parallel acquisition techniques in cardiac cine magnetic resonance imaging using TrueFISP sequences: comparison of image quality and artifacts.** *J Magn Reson Imaging* 2004;20:506–11
16. Ruel L, Brugieres P, Luciani A, et al. **Comparison of in vitro and in vivo MRI of the spine using parallel imaging.** *AJR Am J Roentgenol* 2004;182:749–55
17. Vogt FM, Antoch G, Hunold P, et al. **Parallel acquisition techniques for accelerated volumetric interpolated breath-hold examination magnetic resonance imaging of the upper abdomen: assessment of image quality and lesion conspicuity.** *J Magn Reson Imaging* 2005;21:376–82
18. Price RR, Axel L, Morgan T, et al. **Quality assurance methods and phantoms for magnetic resonance imaging: report of AAPM nuclear magnetic resonance Task Group No. 1.** *Med Phys* 1990;17:287–95
19. Firbank MJ, Coulthard A, Harrison RM, et al. **A comparison of two methods for measuring the signal to noise ratio on MR images.** *Phys Med Biol* 1999;44:N261–264
20. Reeder SB, Wintersperger BJ, Dietrich O, et al. **Practical approaches to the evaluation of signal-to-noise ratio performance with parallel imaging: application with cardiac imaging and a 32-channel cardiac coil.** *Magn Reson Med* 2005;54:748–54
21. Yamada K, Kizu O, Mori S, et al. **Brain fiber tracking with clinically feasible diffusion-tensor MR imaging: initial experience.** *Radiology* 2003;227:295–301
22. Nagee-Poetscher LM, Jiang H, Wakana S, et al. **High-resolution diffusion tensor imaging of the brain stem at 3 T.** *AJNR Am J Neuroradiol* 2004;25:1325–30
23. Kingsley PB, Monahan WG. **Contrast-to-noise ratios of diffusion anisotropy indices.** *Magn Reson Med* 2005;53:911–18
24. Alexander AL, Hasan K, Kindlmann G, et al. **A geometric analysis of diffusion tensor measurements of the human brain.** *Magn Reson Med* 2000;44:283–91